



A novel near-infrared fluorescent probe for detection of hypobromous acid and its bioimaging applications

Wangbo Qu^{a,b}, Xiaoyu Zhang^b, Yingying Ma^b, Fabiao Yu^{a,*}, Heng Liu^{a,b,*}

^a Institute of Functional Materials and Molecular Imaging, College of Clinical Medicine, Key Laboratory of Hainan Trauma and Disaster Rescue, College of Emergency and Trauma, Hainan Medical University, Haikou 571199, PR China

^b Hubei Collaborative Innovation Center for Advanced Organic Chemical Materials, Ministry of Education Key Laboratory for the Synthesis and Application of Organic Functional Molecules & College of Chemistry and Chemical Engineering, Hubei University, Wuhan 430062, PR China

ARTICLE INFO

Article history:

Received 4 May 2019

Received in revised form 17 May 2019

Accepted 5 June 2019

Available online 6 June 2019

Keywords:

Dicyanomethylene benzopyran derivative

HOBr detection

Near-infrared

Fluorescence on-off

Bioimaging

ABSTRACT

Hypobromous acid (HOBr) is an important reactive oxygen species and has been recently found to be associated with a variety of diseases. However, owing to a lack of effective analytical tools, there is still limited understanding of its roles in living systems. Here, we present a new type of near-infrared fluorescent probe DCSN for HOBr detection. The designed probe exhibits high sensitivity with a low detection limit, excellent selectivity over other interfering species and low cytotoxicity. More interestingly, the fluorescence response behavior of the probe was different from the previous literatures due to the intramolecular charge transfer process. Moreover, we have successfully monitored HOBr in living cells by utilizing DCSN. This probe has potential to be used as a promising tool for better understanding the physiological functions of HOBr.

© 2019 Elsevier B.V. All rights reserved.

1. Introduction

Hypobromous acid (HOBr), as a highly potent reactive oxygen species (ROS), has drawn a lot of attention due to its roles in human immune-defenses system and antibacterial effect [1]. Similar to hypochlorous acid (HOCl), endogenous HOBr is produced by the reaction of bromide ion (Br^-) and hydrogen peroxide (H_2O_2) in the presence of peroxidase, such as eosinophil peroxidase (EPO) or myeloperoxidase (MPO) [2,3]. More recent investigations indicate that a certain amount of HOBr in the host immune system can effectively resist pathogens invasion [4]. Aberrant accumulation of HOBr in vivo can cause host tissue damage, which have been involved in multiple diseases, including rheumatoid arthritis [5], kidney diseases [6], cancer [7,8], cardiovascular diseases, neurodegenerative Parkinson's and Alzheimer's diseases [9]. Very recently, Hudson and co-workers further demonstrated that HOBr via oxidation of Br^- could effectively promoted sulfilimine-crosslink formation in collagen IV scaffolds that was found in all basement membranes [10]. As the complicated biological roles of HOBr have been gradually found, there is still a lack of available

probes to detect HOBr in biological system. Thereby, development of effective fluorescent probes for imaging HOBr in living system is imperative to get a view of biological effects of HOBr.

The blood plasma level of Br^- (2–100 μM) is one thousandth of that of Cl^- (100–140 mM) [11,12]. Therefore, the concentration levels of endogenous HOBr producing from Br^- is lower than HOCl [13]. However, the electrophile reactivity of HOBr is significantly better than HOCl [14]. In recent years, fluorescent probes were currently receiving more attention due to its advantages of fast response, high sensitivity and noninvasive detection [15–17]. To date, only very limited of fluorescent probes for HOBr have been constructed in the past few years [18–23]. Among these probes, Han et al reported two series of reversible fluorescent probes for HOBr/AA (ascorbic acid) and HOBr/ H_2S by oxidation-reduction reaction [22,23]. Tang et al reported another two off-on fluorescent probes for HOBr via HOBr-catalyzed coupling reaction of the S-methyl and $-\text{NH}_2$ [20,21]. It is well known that near-infrared (NIR) fluorescent probes showed the following merits in comparison with UV-visible probes: deeper tissue penetration, minimal background interference and less photodamage [24–27]. Enlightened by the above considerations, we herein reported the development and application of a novel near-infrared (NIR) fluorescent probe DCSN for the determination of HOBr in living cells. Surprisingly, the probe exhibited fluorescence on-off response to HOBr. The fluorescence response behavior was different from the reported literatures by Tang et al. Notably, the probe could be successfully used for HOBr detection in living cells.

* Corresponding author at: Hainan Medical University, Haikou 571199, PR China; Hubei University, Wuhan 430062, PR China.

E-mail addresses: fbyu@yic.ac.cn, liuheng11b@hubu.edu.cn (H. Liu).

2. Experimental section

2.1. Reagents and apparatus

All reagents and solvents for the experiments were purchased from commercial suppliers and used without further purification. All the reactions were monitored by thin-layer chromatography (TLC) using UV light. ^1H NMR and ^{13}C NMR were determined on a BRUKER 400 MHz spectrometer. Bruker ultrafleXtreme MALDI-TOF/TOF and ESI-TOF were used for the mass analysis. Ultrapure water (18.2 M cm^{-1}) was used to prepare all solutions in this work. UV-vis absorption spectra were performed on an Agilent Technologies Cary 60. Fluorescence spectra were measured on using 1 cm quartz cuvette on an Agilent Cary Eclipse fluorescence spectrophotometer. Confocal images of HOBr in MCF-7 cells were carried out on Olympus FV1000 laser scanning confocal microscope. HOBr used in this work was prepared and quantitated according to a known method [28]. The pH of the solution was adjusted with a solution of NaOH or HCl (1.0 M). The fluorescence excitation wavelength was 480 nm with excitation and emission slits of 5 nm.

2.2. Cell culture and fluorescence imaging

MCF-7 cells were cultured in DMEM medium supplemented with 10% (v/v) fetal bovine serum and penicillin/streptomycin ($100\text{ }\mu\text{g/ml}$) in an atmosphere of 5% CO_2 at $37\text{ }^\circ\text{C}$. The cytotoxicity of DCSN with different concentrations by using a standard CCK-8 assay [29–31]. In the experiment of imaging of HOBr in living cells, MCF-7 cells were incubated with DCSN ($10\text{ }\mu\text{M}$) for 30 min at $37\text{ }^\circ\text{C}$, and then further treated with HOBr ($100\text{ }\mu\text{M}$), NaBr ($100\text{ }\mu\text{M}$), *N*-acetylcysteine ($20\text{ }\mu\text{M}$)/NaBr ($100\text{ }\mu\text{M}$) or H_2O_2 ($100\text{ }\mu\text{M}$)/NaBr ($100\text{ }\mu\text{M}$) for 30 min. The cells were washed with PBS buffer for three times before subjecting to fluorescence imaging measurements with laser scanning confocal microscope. Emission was collected at red channel (600–700 nm) with 488 nm excitation.

2.3. Synthesis of DCM-NH₂-Br

To a toluene (10 ml) solution of 2-(2-methyl-4H-chromen-4-ylidene) malononitrile (150 mg, 0.72 mmol) and *N*-(2-bromo-4-formylphenyl) acetamide (170 mg, 0.67 mmol) were added piperidine (0.15 ml) and acetic acid (0.15 ml). The reaction mixture was heated and refluxed under Ar for 6 h. After filtration, conc. HCl and EtOH (v/v 2/1, 30 ml) were added to the obtained solid, the reaction mixture was refluxed for 5 h, followed by quenching with saturated aqueous solution of NaHCO_3 . The organic phase was extracted with ethyl acetate, washed with brine, dried over Na_2SO_4 and concentrated under reduced pressure. The residue was purified by flash column chromatography on silica gel (eluent: dichloromethane) to afford DCM-NH₂-Br (113 mg, 43%) as a dark-red solid. ^1H NMR (400 MHz, d_6 -DMSO): δ 8.69 (d, J =

8.2 Hz, 1H), 7.90–7.84 (m, 2H), 7.71 (d, J = 8.3 Hz, 1H), 7.59–7.55 (m, 2H), 7.47 (d, J = 7.7 Hz, 1H), 7.19 (d, J = 15.8 Hz, 1H), 6.87 (s, 1H), 6.81 (d, J = 8.4 Hz, 1H), 6.09 (s, 2H); ^{13}C NMR (100 MHz, d_6 -DMSO): δ 159.1, 152.7, 152.0, 148.3, 138.6, 135.2, 132.8, 129.3, 126.0, 124.6, 124.3, 118.9, 117.5, 117.1, 116.2, 115.0, 114.6, 107.4, 105.4, 58.4; HRMS: Calcd for $\text{C}_{20}\text{H}_{12}\text{BrN}_3\text{O}$ [M^+] 389.0164, found 389.0153.

2.4. Synthesis of DCSN

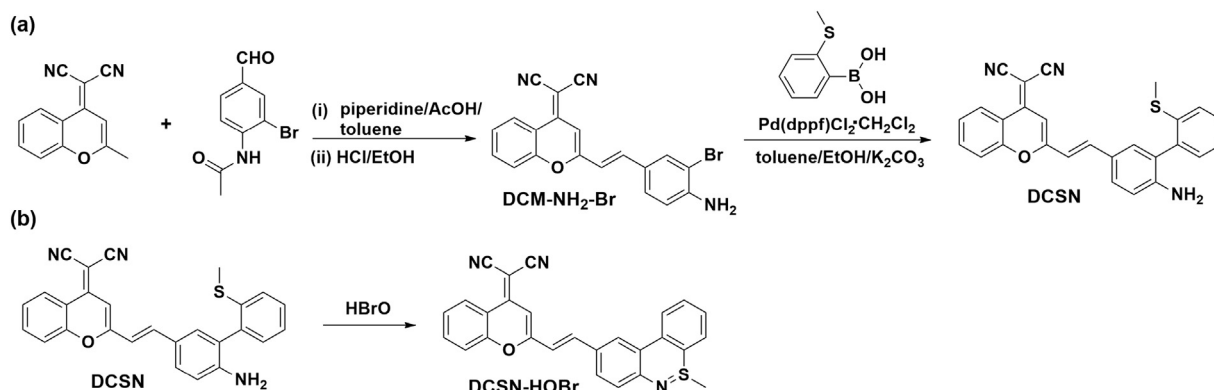
A mixture of DCM-NH₂-Br (50 mg, 0.128 mmol), 2-methylthiophenylboronic acid (28 mg, 0.167 mmol), Pd(dppf)₂Cl₂·CH₂Cl₂ (8 mg, 0.01 mmol), K₂CO₃ (4 M, 2 ml), EtOH (0.6 ml) and toluene (5 ml) were charged into a tube. The reaction mixture was heated at $80\text{ }^\circ\text{C}$ for 24 h under Ar. After removing the solvent under reduced pressure, the residue was purified by flash column chromatography on silica gel (eluent: dichloromethane) to afford DCSN (21 mg, 38%) as a reddish-brown solid. ^1H NMR (400 MHz, d_6 -DMSO): δ 8.70 (d, J = 8.2 Hz, 1H), 7.87 (t, J = 7.6 Hz, 1H), 7.73 (d, J = 8.3 Hz, 1H), 7.66 (d, J = 15.8 Hz, 1H), 7.56 (t, J = 7.7 Hz, 1H), 7.50 (d, J = 7.8 Hz, 1H), 7.44–7.37 (m, 3H), 7.25 (t, J = 7.2 Hz, 1H), 7.18–7.14 (m, 2H), 6.87 (s, 1H), 6.79 (d, J = 8.4 Hz, 1H), 5.36 (s, 2H), 2.37 (s, 3H); ^{13}C NMR (100 MHz, d_6 -DMSO): δ 160.1, 153.1, 152.5, 149.3, 140.8, 138.8, 136.6, 135.5, 131.9, 130.7, 130.6, 129.0, 126.4, 125.4, 125.3, 125.0, 124.8, 123.3, 119.4, 118.2, 117.7, 116.8, 115.3, 113.6, 105.4, 58.0, 15.1; HRMS: Calcd for $\text{C}_{27}\text{H}_{19}\text{N}_3\text{OS}$ [M^+] 433.1249, found 433.1238.

3. Results and discussion

3.1. Probe synthesis and design

Dicyanomethylene benzopyran derivative (DCM-NH₂), a well-known fluorophore with emission in NIR region, was chosen owing to its outstanding spectroscopic properties, such as large stoke shift, excellent photostability [32]. In the design, DCSN was synthesized by a two-step reaction with the overall reaction yield of 16% as shown in Scheme 1a. 2-methylthiophenyl moiety was attached to DCM-NH₂ through Pd-catalyzed Suzuki coupling reaction. The structures of DCM-NH₂-Br and DCSN were well characterized by ^1H NMR, ^{13}C NMR and HRMS analysis.

DCSN, a typical donor- π -acceptor molecule, exhibited strong fluorescence with a peak at 655 nm due to the intramolecular charge transfer (ICT) process. As expected, the sensing products between DCSN and HOBr only emitted weak fluorescence. Perhaps the reason for this was that ICT process of DCSN-HOBr was blocked because of losing the electron donating -NH₂ group. Moreover, HOBr-triggered coupling reaction of the *S*-methyl and -NH₂ have been well documented in the previous literatures [10,18–21]. Thus, we speculated that HOBr was first attacked by *S*-methyl nucleophile of DCSN to generate the bromosulfonium (*S*-Br) intermediate and then formed the final cyclization product sulfilimine (S=N). To further verify the presumption, the reaction



Scheme 1. Synthesis of the target fluorescent probe DCSN (a) and the reaction mechanism of DCSN with HOBr.

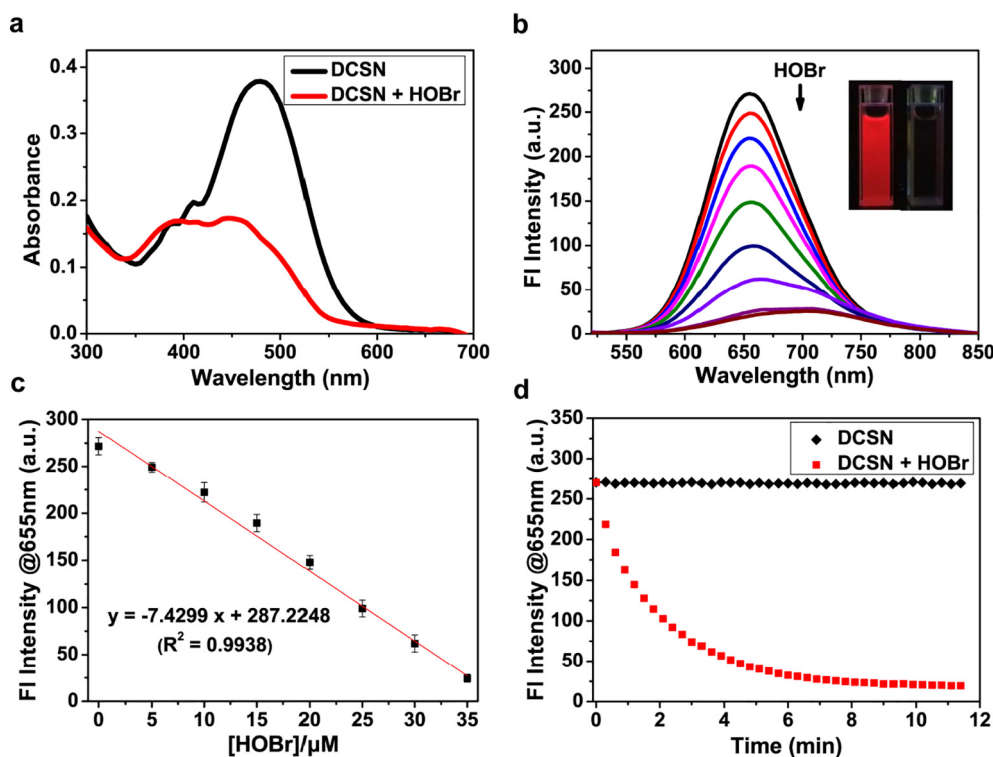


Fig. 1. (a) UV-vis absorption spectra of DCSN (10 μM) before and after addition of HOBr (50 μM). (b) Titration graph of DCSN (10 μM) upon gradual addition of various amounts (0–40 μM). Inset (b): photographs of DCSN without or with HOBr under UV irradiation. (c) Fluorescence intensities at 655 nm of DCSN (10 μM) versus HOBr concentrations (0–35 μM). (d) Time dependent fluorescence measures of DCSN (10 μM) before and after treatment with HOBr (50 μM).

mixture of DCSN with HOBr was confirmed by ESI-MS analysis (Fig. S7). In ESI-MS spectrum, a dominant peak located at m/z 432.1161 corresponded to $[\text{DCSN-HOBr-H}]^+$, which provided the strong evidence for the proposed sensing mechanism in Fig. S8.

3.2. Spectra properties of DCSN

After obtaining DCSN, the photophysical properties were primarily investigated in 10 mM PBS buffer- CH_3CN (3: 2, v/v, pH 7.4) at 25 $^\circ\text{C}$. As illustrated in Fig. 1a, the probe displayed an absorption peak centered at 478 nm. With addition of HOBr, the peak at 478 nm sharply decreased and two new peaks located at 392 nm and 448 nm appeared, suggesting that the structure of DCSN has been changed. Fluorescence emission spectra of DCSN showed a maximum peak at 655 nm under the excitation at 480 nm in absence of HOBr. Upon addition of HOBr to the

solution of DCSN, a gradual fluorescence decrease was observed, which was accompanied by the red-shift of emission peak from 655 nm to 700 nm and fluorescence color changes from red to colorless (Fig. 1b). The decrease in fluorescence intensities was attributed to the formation of compound DCSN-HOBr by HOBr-triggered cyclization reaction of the *S*-methyl and $-\text{NH}_2$. When 40 μM of HOBr was added, approximately 14-fold fluorescence intensity of DCSN decrease was obtained (Fig. S10). Additionally, the fluorescence intensities at 655 nm were linearly proportional to the concentrations of HOBr over a range from 0 μM to 35 μM (linear equation: $y = -7.4299x + 287.2248$, $R^2 = 0.9938$). Subsequently, the detection limit was estimated to be 660 nM according to the eq. $\text{DL} = 3\sigma/k$ (Fig. 1c). Hence, DCSN can be applied to detect HOBr with high sensitivity. The photostability and response kinetics of DCSN were also investigated. As illustrated in Fig. 1d, no detectable fluorescence changes of DCSN

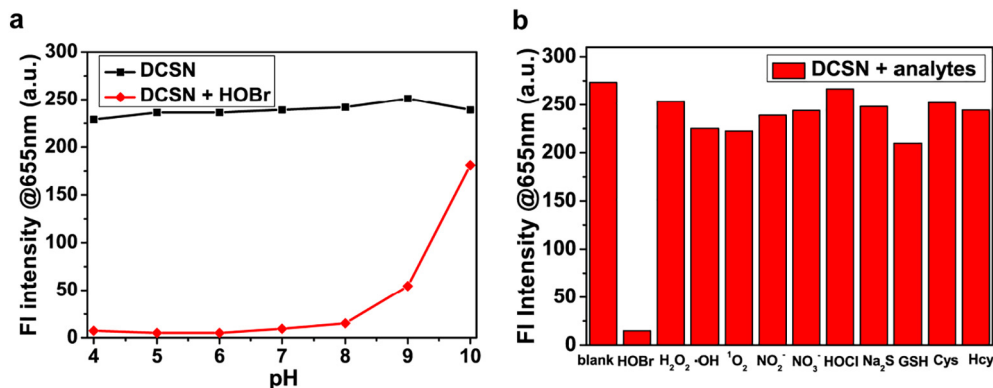


Fig. 2. (a) pH effect on the fluorescence intensities at 655 nm of DCSN (10 μM) in the absence and presence of HOBr (50 μM). (b) Selective fluorescence response of DCSN toward common physiological ROS, RNS and RSS analytes. 50 μM for HOBr, 500 μM for H_2O_2 , $\cdot\text{OH}$, $^1\text{O}_2$, NO_2 , NO_3 , 200 μM for HClO , 100 μM for Na_2S , 1 mM for GSH and 300 μM for Cys, Hcy.

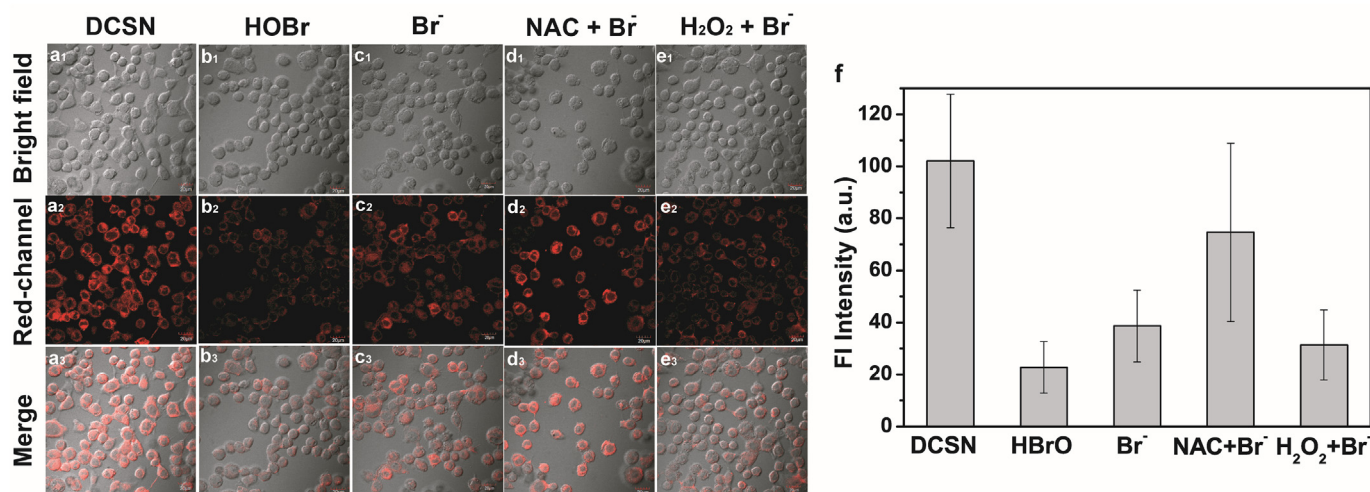


Fig. 3. Bright field (top row), red channel (second row), merged (third row) images of MCF-7 cells incubated with (10 μ M) for 30 min, and then further treated with (a) nothing, (b) HOBr (100 μ M), (c) NaBr (100 μ M), (d) *N*-acetylcysteine (20 μ M)/NaBr (100 μ M) and (e) H₂O₂ (100 μ M)/NaBr (100 μ M) for 30 min, respectively. (f) Fluorescence intensity of cells in panels (f) to (j). $\lambda_{\text{ex}} = 488$ nm, $\lambda_{\text{em}} = 600\text{--}700$ nm, scale bar = 20 μ m.

was observed under the excitation of 480 nm, suggesting the excellent photostability. The fluorescence intensities of DCSN gradually decreased in the presence of HOBr and levelled off within about 8 min.

Furthermore, the effect of pH on the response of DCSN toward HOBr was evaluated. The free DCSN was stable in the pH range from 4.0 to 10.0, while the addition of HOBr resulted in a drastic decrease in the fluorescence intensities over the pH 4.0–8.0 range (Fig. 2a). Due to acid-base neutralization reaction, the fluorescence intensities of DCSN only changed slightly in the pH 9.0–10.0 range before and after the addition of HOBr. From the results obtained, it was inferred that DCSN was a good candidate for sensing of HOBr under simulated physiological conditions. Next, the selectivity of DCSN toward HOBr was examined. As seen in Fig. 2b, only the addition of HOBr elicited a significant change of the fluorescence intensity of DCSN. Other relevant ROS, RNS and RSS analytes including H₂O₂, \cdot OH, ¹O₂, HOCl, NO₂⁻, NO₃⁻, H₂S, GSH, Cys and Hcy only resulted in a very slight fluorescence response (Figs. 2b and S11). Interestingly, although the chemical properties of HOCl were similar to HOBr, fluorescence response behavior was obviously different due to different reaction pathways (Fig. S9). In addition, common biological amino acids and cations such as Phe, Met, Ser, His, Gly, Thr, Glu, Pro, Arg, Lys, Asp, K⁺, Na⁺, Mg²⁺, Ca²⁺, Cu²⁺, Zn²⁺, Fe²⁺ and Fe³⁺ did not trigger obvious fluorescence decreases, even at high concentrations up to 1 mM (Fig. S12). The results showed DCSN was a highly selective on-off fluorescent probe for detection of HOBr over other biological interfering analytes.

3.3. Cell imaging

Encouraged by the excellent performance, we further explored the potential utility of DCSN for fluorescence imaging of HOBr in living cells. Before that, cytotoxicity measurements of DCSN was evaluated using MCF-7 cells by CCK-8 assays, which revealed that DCSN was found to be no obvious cytotoxicity for living cells (Fig. S13). As demonstrated in Fig. 3, DCSN-loaded MCF-7 cells displayed strong fluorescence signals in the red channel. After the cells were incubated with HOBr, a significant decrease of intracellular fluorescence was observed. Importantly, when the cells were pretreated with Br⁻ and then incubated with DCSN, the cells exhibited a rather weak fluorescence. However, upon adding *N*-acetylcysteine (a scavenger of HOBr) to Br⁻-pretreated cells followed by the addition of DCSN, the cells showed a brighter fluorescence than Br⁻ and DCSN-treated cells. In addition, the cells pretreated with Br⁻ and H₂O₂ also resulted in a significantly decreased fluorescence. These results supported that HOBr could be

produced by Br⁻ or Br⁻/H₂O₂, and demonstrated that DCSN could be applied for imaging HOBr in living cells.

4. Conclusion

In summary, by introducing 2-methylthiopheny group to DCM-NH₂ dye, we have successfully designed a new type of on-off fluorescent probe for HOBr with the emission in near-infrared region. The resultant naked eye probe DCSN could well distinguish HOBr from other relevant ROS, RNS and RSS analytes with a low detection limit of 660 nM. Particularly, the probe have been proved to be capable of sensing of HOBr in living cells. We believed that the discovery of DCSN would further broaden the probe design strategy for HOBr.

Acknowledgement

This work was supported by the National Natural Science Foundation of China (NSFC.21602051).

Appendix A. Supplementary data

Supplementary data to this article can be found online at <https://doi.org/10.1016/j.saa.2019.117240>.

References

- [1] D.I. Pattison, M.J. Davies, Kinetic analysis of the reactions of hypobromous acid with protein components: implications for cellular damage and use of 3-bromotyrosine as a marker of oxidative stress, *Biochemistry* 43 (2004) 4799–4809.
- [2] S.J. Klebanoff, Myeloperoxidase: friend and foe, *J. Leukoc. Biol.* 77 (2005) 598–625.
- [3] P.G. Furtmüller, U. Burner, G. Regelsberger, C. Obinger, Spectral and kinetic studies on the formation of eosinophil peroxidase compound I and its reaction with halides and thiocyanate, *Biochemistry* 39 (2000) 15578–15584.
- [4] M.J. Davies, C.L. Hawkins, D.I. Pattison, M.D. Rees, Mammalian heme peroxidases: from molecular mechanisms to health implications, *Antioxid. Redox Signal.* 10 (2008) 1199–1234.
- [5] S.L. Archer, Mitochondrial dynamics - mitochondrial fission and fusion in human diseases, *New. Engl. J. Med.* 369 (2013) 2236–2251.
- [6] K.L. Brown, C. Darris, K.L. Rose, O.A. Sanchez, H. Madu, J. Avance, et al., Hypohalous acids contribute to renal extracellular matrix damage in experimental diabetes, *Diabetes* 64 (2015) 2242–2253.
- [7] C. Gorrini, I.S. Harris, T.W. Mak, Modulation of oxidative stress as an anticancer strategy, *Nat. Rev. Drug Discov.* 12 (2013) 931–947.
- [8] R.A. Cairns, I.S. Harris, T.W. Mak, Regulation of cancer cell metabolism, *Nat. Rev. Cancer* 11 (2011) 85–95.
- [9] Y.W. Yap, M. Whiteman, N.S. Cheung, Chlorinative stress: an under appreciated mediator of neurodegeneration? *Cell. Signal.* 19 (2007) 219–228.

- [10] A.S. McCall, C.F. Cummings, G. Bhavre, R. Vanacore, A. Page-McCaw, B.G. Hudson, Bromine is an essential trace element for assembly of collagen IV scaffolds in tissue development and architecture, *Cell* 157 (2014) 1380–1392.
- [11] H.A. Olszowy, J. Rossiter, J. Hegarty, P. Geoghegan, Background levels of bromide in human blood, *J. Anal. Toxicol.* 22 (1998) 225–230.
- [12] P.G. Furtmüller, U. Burner, C. Obinger, Reaction of myeloperoxidase compound I with chloride, bromide, iodide, and thiocyanate, *Biochemistry* 37 (1998) 17923–17930.
- [13] F.X.R. van Leeuwen, B. Sangster, A.G. Hildebrandt, The toxicology of bromide ion, *Crit. Rev. Toxicol.* 18 (1987) 189–213.
- [14] V.F. Ximenes, N.H. Morgon, A.R. de Souza, Hypobromous acid, a powerful endogenous electrophile: experimental and theoretical studies, *J. Inorg. Biochem.* 146 (2015) 61–68.
- [15] H. Liu, M.N. Radford, C.T. Yang, W. Chen, M. Xian, Inorganic hydrogen polysulfides: chemistry, chemical biology and detection, *Br. J. Pharmacol.* 176 (2019) 616–627.
- [16] W. Chen, A. Pacheco, Y. Takano, J.J. Day, K. Hanaoka, M. Xian, A single fluorescent probe to visualize hydrogen sulfide and hydrogen polysulfides with different fluorescence signals, *Angew. Chem. Int. Ed.* 55 (2016) 9993–9996.
- [17] W. Chen, E.W. Rosser, T. Matsunaga, A. Pacheco, T. Akaike, M. Xian, The development of fluorescent probes for visualizing intracellular hydrogen polysulfides, *Angew. Chem. Int. Ed.* 54 (2015) 13961–13965.
- [18] C. Ma, M. Ma, Y. Zhang, X. Zhu, L. Zhou, R. Fang, X. Liu, H. Zhang, Lysosome-targeted two-photon fluorescent probe for detection of hypobromous acid in vitro and in vivo, *Spectrochim. Acta A Mol. Biomol. Spectrosc.* 212 (2019) 48–54.
- [19] H. Huang, Y. Tian, A ratiometric fluorescent probe for bioimaging and biosensing of HBrO in mitochondria upon oxidative stress, *Chem. Commun.* 54 (2018) 12198–12201.
- [20] X. Liu, A. Zheng, D. Luan, X. Wang, F. Kong, L. Tong, K. Xu, B. Tang, High-quantum-yield mitochondria-targeting near-infrared fluorescent probe for imaging native hypobromous acid in living cells and in vivo, *Anal. Chem.* 89 (2017) 1787–1792.
- [21] K. Xu, D. Luan, X. Wang, B. Hu, X. Liu, F. Kong, B. Tang, An ultrasensitive cyclization-based fluorescent probe for imaging native HOBr in live cells and zebrafish, *Angew. Chem. Int. Ed.* 55 (2016) 12751–12754.
- [22] B. Wang, P. Li, F. Yu, J. Chen, Z. Qu, K. Han, A near-infrared reversible and ratiometric fluorescent probe based on Se-BODIPY for the redox cycle mediated by hypobromous acid and hydrogen sulfide in living cells, *Chem. Commun.* 49 (2013) 5790–5792.
- [23] F. Yu, P. Song, P. Li, B. Wang, K. Han, Development of reversible fluorescence probes based on redox oxoammonium cation for hypobromous acid detection in living cells, *Chem. Commun.* 48 (2012) 7735–7737.
- [24] R.R. Nawimanager, B. Prasai, S.U. Hettiarachchi, R.L. McCarley, Cascade reaction-based, near-infrared multiphoton fluorescent probe for the selective detection of cysteine, *Anal. Chem.* 89 (2017) 6886–6892.
- [25] W. Chen, S. Xu, J.J. Day, D. Wang, M. Xian, A general strategy for development of near-infrared fluorescent probes for bioimaging, *Angew. Chem. Int. Ed.* 56 (2017) 16611–16615.
- [26] K. Gu, Y. Liu, Z. Guo, C. Lian, C. Yan, P. Shi, H. Tian, W.H. Zhu, In situ ratiometric quantitative tracing of intracellular leucine aminopeptidase activity via an activatable near-infrared fluorescent probe, *ACS Appl. Mater. Interfaces* 8 (2016) 26622–26629.
- [27] D. Yu, F. Huang, S. Ding, G. Feng, Near-infrared fluorescent probe for detection of thiophenols in water samples and living cells, *Anal. Chem.* 86 (2014) 8835–8841.
- [28] K. Kumar, D.W. Margerum, Kinetics and mechanism of general-acid-assisted oxidation of bromide by hypochlorite and hypochlorous acid, *Inorg. Chem.* 26 (1987) 2706–2711.
- [29] F. Chen, J. Zhang, W. Qu, X. Zhong, H. Liu, J. Ren, H. He, X. Zhang, S. Wang, Development of a novel benzothiadiazole-based fluorescent turn-on probe for highly selective detection of glutathione over cysteine/homocysteine, *Sens. Actu. B-Chem.* 266 (2018) 528–533.
- [30] Z. Chen, X. Zhong, W. Qu, T. Shi, H. Liu, H. He, X. Zhang, S. Wang, A highly selective HBT-based “turn-on” fluorescent probe for hydrazine detection and its application, *Tetrahedron Lett.* 58 (2017) 2596–2601.
- [31] Y. Lv, P. Liu, H. Ding, Y. Wu, Y. Yan, H. Liu, X. Wang, F. Huang, Y. Zhao, Z. Tian, Conjugated polymer-based hybrid nanoparticles with two-photon excitation and near-infrared emission features for fluorescence bioimaging within the biological window, *ACS Appl. Mater. Interfaces* 7 (2015) 20640–20648.
- [32] W. Zhang, F. Huo, C. Yin, Recent advances of dicyano-based materials in biology and medicine, *J. Mater. Chem. B* 6 (2018) 6919–6929.